Electrical conduction of silicon oxide containing silicon quantum dots

2006 J. Phys.: Condens. Matter 18 9943

(http://iopscience.iop.org/0953-8984/18/43/016)

INSTITUTE OF PHYSICS PUBLISHING JOURNAL OF PHYSICS: CONDENSED MATTER

J. Phys.: Condens. Matter **18** (2006) 9943–9950 doi:10.1088/0953-8984/18/43/016

Electrical conduction of silicon oxide containing silicon quantum dots

X D Pi[1,3], O H Y Zalloum[1], A P Knights[1], P Mascher[1] and P J Simpson[2]

[1] Department of Engineering Physics, McMaster University, Hamilton, ON, L8S 4L7, Canada
[2] Department of Physics and Astronomy, University of Western Ontario, London, ON, N6A 3K7, Canada

E-mail: xdpi@umn.edu and aknight@univmail.cis.mcmaster.ca

Received 3 April 2006, in final form 27 September 2006
Published 13 October 2006
Online at stacks.iop.org/JPhysCM/18/9943

Abstract

Current–voltage measurements have been made at room temperature on a Si-rich silicon oxide film deposited via electron-cyclotron resonance plasma enhanced chemical vapour deposition (ECR-PECVD) and annealed at 750–1000 °C. The thickness of the oxide between Si quantum dots embedded in the film increases with increasing annealing temperature. This leads to a decreasing current density as the annealing temperature is increased. Assuming the Fowler–Nordheim tunnelling mechanism in large electric fields, we obtain an effective barrier height ϕ_{eff} of $\sim 0.7 \pm 0.1$ eV for an electron tunnelling through an oxide layer between Si quantum dots. The Frenkel–Poole effect can also be used to adequately explain the electrical conduction of the film under the influence of large electric fields. We suggest that at room temperature Si quantum dots can be regarded as traps that capture and emit electrons by means of tunnelling.

1. Introduction

Si quantum dots (QDs) have been showing great promise as the basis for Si light-emitting devices [1, 2]. The quantum efficiency of light emission is significantly increased in Si QDs compared with bulk Si because of the three-dimensional confinement of carriers in small volumes ($<\sim 5$ nm in diameter) that are virtually free of defects. These QDs are usually embedded in a SiO_2 matrix to take advantage of the high quality and stability of the Si/SiO_2 interface. The dielectric nature of SiO_2 requires that Si QDs are generally excited by hot carriers when subjected to electrical pumping [3].

It has been shown that electrons are the dominant carriers in silicon oxide containing Si QDs [4, 5]. The incorporation of Si QDs leads to a conductivity larger than that of SiO_2 [4, 6].

[3] Present address: Department of Mechanical Engineering, University of Minnesota, Minneapolis, MN 55455, USA.

DiMaria *et al* [4] examined all possible mechanisms for charge transport in silicon oxide containing Si QDs, fabricated by annealing Si-rich silicon oxide (SRSO) designated as SiO_x ($x < 2$) with Si atomic concentrations of 34–39% at 1000 °C for 30 min. They concluded that the dominant conduction mechanism appeared to be controlled by the tunnelling of electrons between the QDs. In another study, Maeda *et al* [7] investigated the electrical properties of QDs fabricated by the rapid thermal oxidation of an ultrathin amorphous Si (α-Si:H) film. They found that the charging and consequent screening of the QDs led to N-shaped current (I)–voltage (V) curves. These above examples highlight the complex nature of electrical conduction in silicon oxide containing Si QDs. Despite these and other studies [8, 9], a complete picture has yet to be proposed and fully described.

It is well known that electrons can travel through a thin SiO_2 film by means of direct tunnelling or Fowler–Nordheim tunnelling [10]. Direct tunnelling indicates the presence of a trapezoidal potential barrier whereas Fowler–Nordheim tunnelling takes place when electrons tunnel through a potential barrier that is triangular in shape. Generally speaking, a large electric field is needed to transform a rectangular potential barrier into a triangular potential barrier. Therefore, Fowler–Nordheim tunnelling usually dominates in relatively strong electric fields while direct tunnelling is the main conduction mechanism in weak electric fields. Although tunnelling is regarded as being mainly responsible for charge transport in SiO_2, the Frenkel–Poole effect has also been observed in SiO_2 [11, 12]. The Frenkel–Poole effect relates to the electric field enhanced thermal emission of charge carriers from charged traps [11, 13]. Given the fact that Si QDs can be charged [7], it is possible that they efficiently emit charge carriers in silicon oxide with the help of electric fields.

In the present work I–V measurements were performed at room temperature on an SRSO film with a Si atomic concentration of 40% after annealing at 750-1000 °C. We focus on the electrical conduction of silicon oxide in which Si QDs are already electrically charged. It is found that either the Fowler–Nordheim tunnelling or the Frenkel–Poole effect can be used to explain the electrical conduction in our experiment. We propose that at room temperature Si QDs formed by Si-rich deposition and relatively low-temperature annealing can be regarded as traps that capture and emit electrons by means of tunnelling.

2. Experimental details

An SRSO film with a Si atomic concentration of 40% was grown on a ∼500 μm thick ⟨100⟩ Cz Si substrate (As-doped, n^+-type, 0.0035 Ω cm) at a temperature of 100 °C by electron cyclotron resonance plasma enhanced chemical vapour deposition (ECR-PECVD). The deposition system has been described in detail elsewhere [14]. The thickness and refractive index of the film were determined with an ellipsometer to be 77 nm and 1.68, respectively. The film was cleaved into three samples A, B and C. Each sample was subsequently annealed in a tube furnace with a flowing argon gas ambient for 3 h at 750, 900 and 1000 °C, respectively. All the samples were further annealed at 750 °C for 1 h in the same furnace with a flowing hydrogen gas ambient. Electrical backside contacts were formed via deposition of 200 nm thick Al followed by rapid thermal annealing at 550 °C for 5 min in a nitrogen ambient. The heavy doping of the Si substrate led to an Ohmic Al–Si contact [15]. Finally, 100 nm thick indium tin oxide (ITO) dots with a diameter of 1.2 mm were deposited on the top of the SRSO surface by use of a shadow mask. The centre-to-centre distance between neighbouring ITO dots was 1.9 mm. The sheet resistance of the ITO was ∼100 Ω/□, while the optical transmittance at wavelengths in the near-infrared region was ∼90%. Therefore, each ITO dot acted as a transparent electrode for a single device. A schematic of the device structure is illustrated in figure 1.

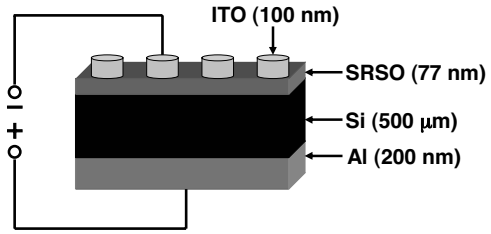

Figure 1. A schematic of the device structure, showing one of the devices under reverse bias. The thickness of each layer in the device structure is indicated in the bracket.

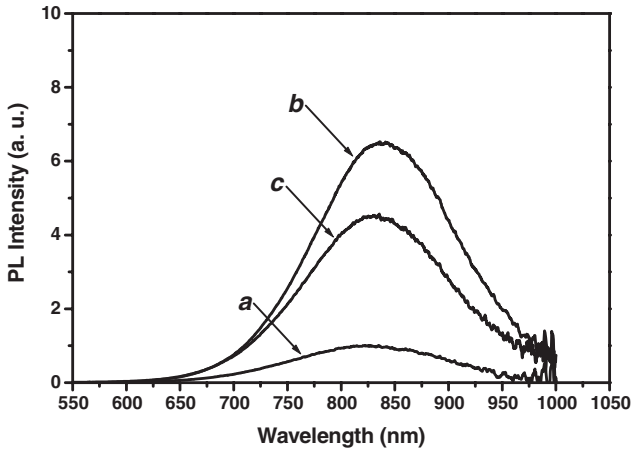

Figure 2. The PL spectra for sample C, which is (a) initially annealed at 1000 °C for 3 h in an argon ambient and (b) further annealed at 750 °C for 1 h in a hydrogen ambient and (c) finally at 550 °C for 5 min in a nitrogen ambient.

Photoluminescence (PL) from each sample was measured at room temperature before the ITO deposition. The PL setup comprised a Cd–He laser operating at a wavelength of 325 nm and an Ocean Optics S2000 spectrometer that featured a high-sensitivity linear CCD array. The effective power density of the laser beam on the surface of the samples was ∼0.64 W cm^{-2}. Room temperature I–V measurements were performed using an Agilent 6624A DC power supply automatically controlled with a Labview graphical user interface (GUI). The voltage was ramped using a step of 0.5 V at a ramp rate of 1.9 V s^{-1}. The I–V curve for each device was derived from the measured voltages for an external series resistor of 100 Ω. The delay time for measurements after each voltage was applied was 5 s. This short delay led to hysteretic N-shaped I–V curves when all the devices were measured for the first time, characteristic of the charging and screening of Si QDs [7]. A second measurement was carried out to obtain the static I–V features immediately after a hysteretic N-shaped I–V curve was measured. The absence of the hysteresis in the second measurement indicated that Si QDs were already charged after the first measurement [7].

3. Results and discussion

The existence of Si QDs in all the samples is evidenced by their PL. Figure 2 shows the PL spectra for sample C after various annealing treatments. These spectra have been corrected

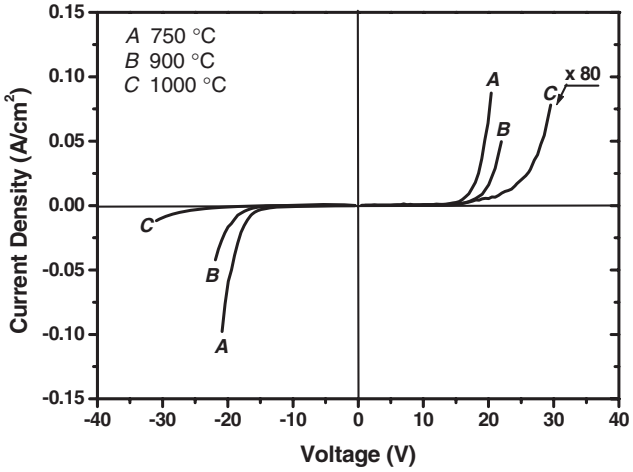

Figure 3. The current density as a function of voltage for samples A, B and C, which are initially annealed in an argon ambient for 3 h at 750, 900 and 1000 °C, respectively. The current density for sample C is shown 80 times larger than measured.

with respect to the system response of our PL setup. Si nanocrystals (Si QDs) whose PL peaks at 827 nm are formed after annealing at 1000 °C in an argon ambient. After hydrogenation at 750 °C the PL intensity increases owing to the hydrogen passivation of non-radiative centres. At the same time the PL peak redshifts to 842 nm, indicating hydrogenation-induced bond distortion [16]. Both the redshift and the increase in PL intensity are partially reversed following annealing at 550 °C in a nitrogen ambient. The underlying mechanism associated with annealing in nitrogen requires further study. It is important to note that after the formation of the nanocrystals during annealing in an argon ambient their size changes only marginally during annealing at 750 °C in a hydrogen ambient and at 550 °C in a nitrogen ambient (this applies to samples A and B also). X-ray diffraction measurements suggest that Si nanocrystals with a characteristic PL peak at 827 nm are 3.5 ± 0.7 nm in diameter.

Much weaker PL signals are observed from samples A and B (not shown). This is caused by the amorphous nature of Si QDs formed at temperatures below the crystallization temperature ∼1000 °C for nanometre-sized Si in silicon oxide [16–19]. Comparing the PL spectra for samples A, B and C we find that the PL peak redshifts with the increase of annealing temperature in an argon ambient. Assuming that quantum confinement is the dominant mechanism for the PL from both amorphous and crystalline Si QDs [18], we conclude that the mean size of the dots in sample B is larger than in sample A, but smaller than in sample C.

No electroluminescence from these samples was detected at room temperature with our Ocean Optics S2000 spectrometer. This does not significantly affect the discussion on the electrical conduction of our silicon oxide film containing Si QDs. The absence of electroluminescence will be addressed subsequently in conjunction with the results derived from the I–V measurements. Figure 3 shows static current density J as a function of voltage V for all the samples, in which Si QDs are already charged. It is seen that J decreases for a given voltage with the increase of annealing temperature in an argon ambient. Assuming a homogeneous distribution of QDs with a negligible size dispersion, we relate the thickness s of oxide between the dots to the size d of the dots, such that $s = (2.9687 \times 10^7/\sqrt[3]{C_{\text{excess}}} - 1)d$, where C_{excess} is the excess Si concentration in cm^{-3} [20]. For our film with a Si atomic concentration of 40% $s = 0.78d$. Therefore, J decreases with increasing s. This is consistent

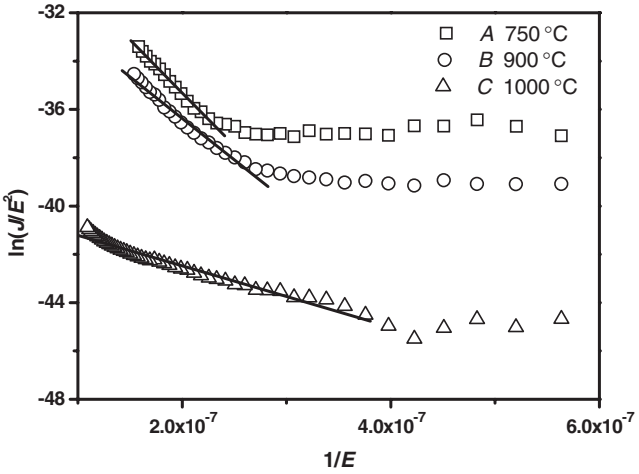

Figure 4. The Fowler–Nordheim plots for samples A, B and C, which are initially annealed in an argon ambient for 3 h at 750, 900 and 1000 °C, respectively. The solid lines are least square fits to the Fowler–Nordheim tunnelling. E and J are in V cm^{-1} and A cm^{-2}, respectively.

with a tunnelling effect, where the probability of tunnelling transmission of electrons decreases with increase in the barrier width (s).

The breakdown voltage of ∼31 V for sample C is larger than those for samples A and B, ∼22 V, as a result of their relative s values. The relatively large reverse bias of 31 V causes the formation of a depletion layer in the near interface region of the Si substrate. The depletion layer width can be up to 10 nm in our case [15], which is large enough to make the tunnelling current density smaller under reverse bias than under forward bias for sample C (figure 3). We further suggest that the corresponding depletion layer in sample A or B below −22 V is not wide enough to generate a rectifying effect.

We assume the Fowler–Nordheim tunnelling mechanism [21] for the electrical conduction in all the samples, in which the current density is given by

$$J = fE^2q^3 \exp[-4(2m^*)^{1/2}\phi^{3/2}/(3\hbar qE)]/(16\pi^2\hbar\phi), \tag{1}$$

where f, E, ϕ, m^* and q are a correction factor, the electric field in the oxide between Si QDs, the barrier height for electrons tunnelling through the oxide between Si QDs, the effective electron mass and the electron charge, respectively. We plot $\ln(J/E^2)$ against $1/E$ under reverse bias in figure 4. In the calculation of E it is presumed that the voltage drops across the ITO, Si QDs and the n^+-type Si substrate, the work function difference between the ITO and n^+-type Si substrate, and the surface potential for the substrate–oxide interface are all relatively small if not negligible. Thus, $E = E_{\rm exp}(d + s)/s$, where $E_{\rm exp}$ is the voltage drop across a device divided by the film thickness of 77 nm. The solid lines are least square fits of the form of equation (1). It is clear that both the critical electric field $E_{\rm FN}$ for the onset of Fowler–Nordheim tunnelling and the Fowler–Nordheim tunnelling current density decrease with the increase of annealing temperature in argon during formation of the Si QDs. This is consistent with the dependence of the Fowler–Nordheim tunnelling on the barrier width s [10]. Electrical conduction in an electric field below $E_{\rm FN}$ is attributed to direct tunnelling.

We calculate the effective barrier height $\phi_{\rm eff}$ to be ∼0.7 ± 0.1 eV by using $E_{\rm FN} =$ 2.5 MV cm^{-1} and $s = 2.7 \pm 0.5$ nm for sample C. We note that $\phi_{\rm eff}$ is smaller than the

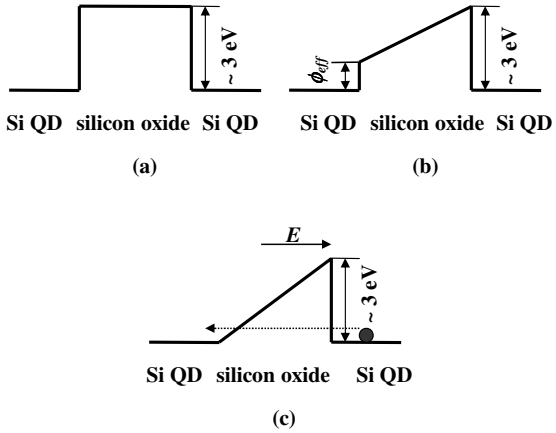

Figure 5. The schematic of energy levels for electrons in silicon oxide containing Si QDs. (a) The original barrier is rectangular with a barrier height of ∼3 eV. (b) The localized electric field induced by the screening effect of charged Si QDs transforms the rectangular barrier to a trapezoidal barrier. (c) The Fowler–Nordheim tunnelling occurs when electrons gain energy to overcome the smaller base ($\phi_{\rm eff}$) of the trapezoidal barrier with the help of the external field E.

barrier height ∼3 eV obtained from photoconductivity and photoionization measurements [4]. Figure 5 schematically shows the energy levels for electrons in the present system. We believe that the screening effect of charged Si QDs gives rise to localized electric fields, transforming the original rectangular barriers (figure 5(a)) into trapeziform barriers (figure 5(b)). For Fowler–Nordheim tunnelling to occur (figure 5(c)) electrons need the help of external fields to overcome the smaller bases of these trapezoids, which are 0.7 eV ± 0.1 eV, similar to the value of 0.6 eV obtained by DiMaria *et al* [4]. It is shown in figure 2 that J very weakly depends on the electric field polarity if the effect of the depletion layer is not considered. This results from the fact that the localized electric fields caused by charged Si QDs change direction with respect to the external electric fields.

Assuming that $\phi_{\rm eff}$ is nearly the same for all the samples, we calculate the values of s to be 1.6 ± 0.2 and 1.9 ± 0.3 nm for samples A and B, respectively. Using these values of s we can estimate the maximum kinetic energy (KE) of an electron as it moves between neighbouring QDs. In the simple one-dimensional case KE $= Eqs$. For samples A and B the maximum KE (determined by the electrical breakdown of the film) is less than 1.5 eV, which is not large enough to excite an electron–hole pair according to the PL data. For sample C, however, where a breakdown field of 9 MV cm^{-1} is achievable, the KE could reach 2.4 eV, presumably enough to cause electroluminescence. The absence of electroluminescence from sample C then appears related to the small current of electrons able to tunnel between neighbouring QDs (figure 3).

We have also considered the Frenkel–Poole effect [11, 13] as a model for charge transport in all the samples, in which the current density is given by

$$J = CE\exp\{-q\psi/(2k_{\rm B}T) + [q^3E/(\pi\varepsilon)]^{1/2}/(2k_{\rm B}T)\}, \tag{2}$$

where C, ψ, $k_{\rm B}$, ε and T are a system-specific constant, the barrier height for electrons to escape from traps, the Boltzmann constant, the dielectric constant of the film and the temperature, respectively. In figure 6 we plot $\ln(J/E)$ against $E^{1/2}$ under reverse bias. The solid lines are least square fits based on the Frenkel–Poole effect. The critical electric field $E_{\rm FP}$ for the beginning of the Frenkel–Poole effect approximates $E_{\rm FN}$ for each sample. Using $\psi_{\rm eff} = qsE_{\rm FP}$, where $\psi_{\rm eff}$ is the effective barrier height for electrons to escape from traps, we estimate from

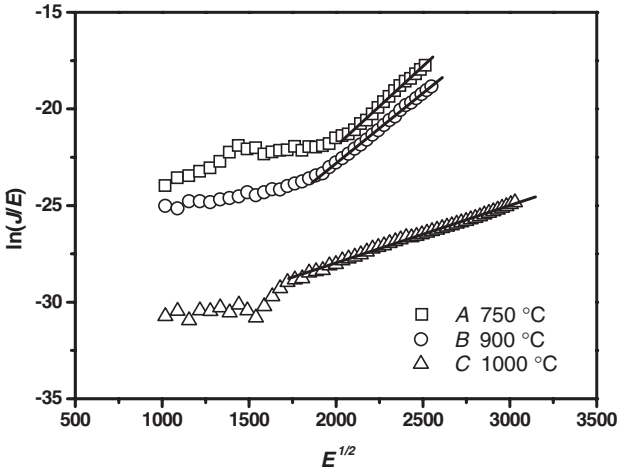

Figure 6. The Frenkel–Poole plots for samples A, B and C, which are initially annealed in an argon ambient for 3 h at 750, 900 and 1000 °C, respectively. The solid lines are least square fits to the Frenkel–Poole effect. E and J are in V cm^{-1} and A cm^{-2}, respectively.

sample C that ψ_{eff} is 0.7 ± 0.1 eV. The same values of ψ_{eff} and ϕ_{eff} indicate that the traps in the Frenkel–Poole model are actually Si QDs, hence it appears that at room temperature Si QDs trap and emit electrons. A trapped electron arrives via tunnelling through the intervening oxide from a neighbouring Si QD, while an emitted electron will tunnel through the oxide to a neighbouring Si QD. Clearly, the whole charge transport process is limited by the emission of electrons. Although the transport process may be explained with either the Frenkel–Poole or the Fowler–Nordheim model, comparison of figures 4 and 6 shows that the experimental data are better fitted with the former. It is well known that the Frenkel–Poole model accurately explains the electrical conduction of a dielectric film with a distribution of traps [11], which is the case in the present study. Given the excellent fit based on the Frenkel–Poole effect, we feel that it is appropriate to describe the charge transport in the present system as trap (Si QD) assisted tunnelling. The refractive index n ($n = \varepsilon^{1/2}$) has been estimated from the slope of each Frenkel–Poole effect fitting. The values of n are 1.74 ± 0.07, 1.85 ± 0.26 and 3.55 ± 1.85 for samples A, B and C, respectively. The Si QD-induced increase in the refractive index of silicon oxide has been observed previously [22]; however, the value of 3.55 for sample C is unrealistic and difficult to estimate with greater accuracy due to the small measured current density.

4. Conclusion

In summary, current–voltage measurements have been made at room temperature on identically deposited silicon-rich silicon oxide (SRSO) films. The thickness of oxide between Si quantum dots (Si QDs) formed by post-deposition annealing was varied via control of the annealing temperature, the separation increasing with the increase of annealing temperature. An increase in Si QD separation leads to a decrease in current density. Assuming the Fowler–Nordheim tunnelling mechanism in large electric fields, we obtain an effective barrier height $\phi_{\text{eff}} \sim 0.7 \pm 0.1$ for an electron tunnelling through an oxide layer between Si QDs. A good agreement with experimental data is also found using the Frenkel–Poole model, which leads us to postulate that charge transport in these films can be regarded as trap (Si QD) assisted tunnelling.

Acknowledgments

The authors thank Dr A Kitai and Mr P Jonasson for assistance in device fabrication. X-ray diffraction measurements were provided courtesy of Dr D Comedi. This work is supported by the Natural Sciences and Engineering Research Council of Canada, Ontario Centers of Excellence Inc., and the Ontario Research and Development Challenge Fund under the Ontario Photonics Consortium.

References

[1] Reed G and Knights A P 2004 *Silicon Photonics: An Introduction* (New York: Wiley)
[2] Ossicini S, Pavesi L and Priolo F 2003 *Light Emitting Silicon for Microphotonics* (New York: Springer)
[3] Franzò G, Irrera A, Moreira E C, Miritello M, Iacona F, Sanfilippo D, Stefano G D, Fallica P G and Priolo F 2002 *Appl. Phys.* A **74** 1
[4] DiMaria D J, Dong D W, Falcony C, Theis T N, Kirtley J R, Tsang J C, Young D R, Pesavento F L and Brorson S D 1983 *J. Appl. Phys.* **54** 5801
[5] DiMaria D J and Arnett P C 1977 *IBM J. Res. Dev.* **21** 227
[6] DiMaria D J, Kirtley J R, Pakulis E J, Dong D W, Kuan T S, Pesavento F L, Theis T N, Cutro J A and Brorson S D 1984 *J. Appl. Phys.* **56** 401
[7] Maeda T, Suzuki E, Sakata I, Yamanaka M and Ishii K 1999 *Nanotechnology* **10** 127
[8] la Torre J D, Souifi A, Lemiti M, Poncet A, Busseret C, Guillot G, Bremond G, Gonzalez O, Garrido B and Morante J R 2003 *Physica* E **17** 604
[9] Castagna M E, Coffa S, Monaco M, Caristia L, Messina A, Mangano R and Bongiorno C 2003 *Physica* E **16** 547
[10] Depas M, Vermeire B, Mertens P W, Meirhaeghe R L V and Heyns M M 1995 *Solid-State Electron.* **38** 1465
[11] Harrella W and Frey J 1999 *Thin Solid Films* **352** 195
[12] Verwey J F 1972 *J. Appl. Phys.* **43** 2273
[13] Frenkel J 1938 *Phys. Rev.* **54** 647
[14] Boudreau M, Boumerzug M, Mascher P and Jessop P E 1993 *Appl. Phys. Lett.* **63** 3014
[15] Sze S M 2002 *Semiconductor Devices Physics and Technology* (New York: Wiley)
[16] Pi X D, Zalloum O H Y, Roschuk T, Wojcik J, Knights A P and Mascher P 2006 *Appl. Phys. Lett.* **88** 103111
[17] Yi L X, Heitmann J, Scholz R and Zacharias M 2002 *Appl. Phys. Lett.* **81** 4248
[18] Molinari M, Rinnert H and Vergnat M 2004 *Europhys. Lett.* **66** 674
[19] Iacona F, Bongiorno C and Spinella C 2004 *J. Appl. Phys.* **95** 3723
[20] Zunger A and Wang L W 1996 *Appl. Surf. Sci.* **102** 350
[21] Lenzlinger M and Snow E H 1969 *J. Appl. Phys.* **40** 278
[22] Pavesi L, Negro L D, Mazzoleni C, Franzò G and Priolo F 2000 *Nature* **408** 440